Front. Earth Sci. 2021, 15(4): 892–908
https://doi.org/10.1007/s11707-020-0836-y

RESEARCH ARTICLE

Influence of sedimentation and diagenesis on reservoir physical properties: a case study of the Funing Formation, Subei Basin, eastern China

Jinkai WANG (✉)[1,2], Yuxiang FU[1], Zhaoxun YAN[1,3], Jialin FU[1], Jun XIE[1,2], Kaikai LI[4], Yongfu ZHAO[4]

1 College of Earth Science and Engineering, Shandong University of Science and Technology, Qingdao 266590, China
2 Laboratory for Marine Mineral Resources, Qingdao National Laboratory for Marine Science and Technology, Qingdao 266237, China
3 The Fourth Gas Production Plant, Changqing Oilfield Branch, PetroChina, Xi'an 710021, China
4 Management Centre of Oil and Gas Exploration, Shengli Oilfield, SINOPEC, Dongying 257000, China

Abstract The sandstone of the third member of the Funing Formation (E_1f_3) in the northern slope zone of the Gaoyou Sag has the typical characteristics of high porosity and ultralow permeability, which makes it difficult for oil to flow. In this study, the lithological characteristics, sedimentary facies, diagenetic characteristics, pore structure, and seepage ability of this sandstone are characterized in detail. Correlation analysis is used to reveal the reason for the sandstone high porosity-low permeability phenomenon in the study area. The results indicate that this phenomenon is controlled mainly by the following three factors: 1) the sedimentary environment is the initial affecting factor, whereby the deposition of a large number of fine-grained materials reduces the primary pores of sandstone. 2) The Funing Formation has undergone strong compaction and cementation, which have led to the removal of most of the primary pores and a reduction in size of the throat channels. 3) Owing to fluid activity during the later stage of diagenesis, sandstone underwent intense dissolution and a large number of particles (feldspar and lithic debris) formed many dissolution pores (accounting for nearly 60% of the total pore space). Among these factors, dissolution has contributed the most to the development of high porosity-low permeability phenomenon. This is mainly attributed to the inhomogeneous dissolution process, whereby the degree of particle dissolution (e.g. feldspar) exceeds that of cementing minerals (clay and carbonate minerals). The secondary dissolution pores have increased the porosity of sandstone in the study area; however, the pore connectivity (permeability) has not been significantly improved, thus resulting in the special high porosity-low permeability characteristics of this sandstone.

Keywords Gaoyou Depression, constant-rate mercury injection, porosity anomaly, diagenesis, sedimentary microfacies

Received May 4, 2020; accepted September 27, 2020

E-mail: wangjk@sdust.edu.cn

1 Introduction

A unified view has been formed in which the rock physical characteristics are generally determined by their sedimentation and diagenesis (Sallam et al., 2019). Sedimentary facies determine the quantity and grain characteristics of sediments, including the clastic particle abundance, type, size, sorting and roundness, which can lead to various reservoir characteristics (Herlinger et al., 2017). For delta front subfacies, the hydrodynamic conditions of the underwater distributary channel are relatively strong; so, the sandstone deposited in this microfacies has a high purity and large grain size, and often has a high porosity and permeability (Hood et al., 2018). However, in a distal fine-grained sedimentation area or in the area between distributary channels, sandstone often has poor physical properties because of its high clay content (Milliken and Olson, 2017; Zhong et al., 2018). Sedimentation which determines sandstone initial pore morphology has a great influence on its primary pore size. The type, size, shape, sorting degree, and other parameters of clastic particles have considerable impact on the primary pores of sandstone (Liu et al., 2019; Usman et al., 2020). Sedimentation also has a certain impact on subsequent diagenesis. First, provenance is an indicator of sediment transport distance, which determines the degree of

transformation of detrital materials. Clastic materials close to the source area are poorly sorted and cannot form a good reservoir; however, the rock pores formed by systematically reformed sediments are generally well sorted and can form a good structure for storing fluid (Zhao et al., 2017). Second, a sedimentary facies belt will lead to a plane difference in sandstone. The thickness, grain size, sorting, and impurity content of sand bodies vary between different sedimentary facies belts. Even within the same belt, the sediment composition can change due to the variation in hydrodynamic conditions, thus producing different physical properties (Zhang et al., 2020). Third, the content of soft particles (e.g. mica, mudstone, phyllite, and other plastic clastic minerals) in the sediment also has a great impact on sandstone physical properties. Soft particles usually fill the pores and reduce the porosity during the later compaction process (Yang et al., 2020). In addition, the grain size and texture maturity of sediments also control the rock's physical properties.

Diagenesis includes compaction, cementation, and dissolution, which directly affect 1) the physical properties of sandstone after consolidation and diagenesis, and 2) the type, content, and micropore structure of cements (Sarkar, 2017). Differences in these parameters result in the formation of sandstone reservoirs with different pore types (Reza, 2018; Yasin et al., 2019). In addition, diagenesis alterations usually have a considerable influence on the changes in porosity and permeability of sandstone, especially tight sandstone (Morad et al., 2010; Lai et al., 2018). For example, compaction and cementation can greatly reduce the porosity and permeability of sandstone (Shalaby et al., 2014; Lai et al., 2017). Carbonate minerals are the main cementing material and are primarily distributed in the sandstone-mudstone contact zone. They exhibit significant negative correlations with physical parameters (porosity and permeability) and the rock storage space volume (Dillinger et al., 2014). Other cementing materials that decrease the porosity and permeability of a reservoir are clay minerals formed by mechanical and chemical deposition; these components can fill the primary pores of sandstone to the greatest extent, thus degrading the physical properties of a rock (Wu et al., 2017). Generally, the higher the sandstone clay mineral content, the lower its porosity. However, this correlation may change if the content of soluble clay minerals in sandstone increases (Aoyagi and Kazama, 1980). For example, the kaolinite content of sandstone may be positively correlated with its porosity because kaolinite dissolves and is transformed into other minerals under certain conditions, thereby increasing the reservoir porosity (Arostegui et al., 2006). The content of plastic cuttings in sandstone has a considerable influence on its physical properties. In the early diagenetic stage, these cuttings are easily contracted after compaction, which significantly reduces the porosity of sandstone (Liu et al., 2020). Compaction and cementation can occur in all periods of diagenesis; however, the early stage usually has a greater influence on the porosity of sandstone than any other stage (Yang et al., 2012). For instance, the initial compaction and cementation can significantly reduce the porosity of sandstone, even up to 80% (MacFadden et al., 2015; Glombitza et al., 2016; Qian et al., 2019). In contrast, cementation during the late diagenesis stage (e.g. quartz and pyrite precipitate cementation) is usually of a relatively small scale with little effect on the physical properties, reducing porosity by 1%–20% (Net et al., 2002). Dissolution occurs during or after compaction and cementation, which can reverse the rapid decreases in porosity and permeability (Spotl et al., 1993; Ballas et al., 2018). Dissolution often occurs in particles such as plagioclase, alkaline feldspar, and metamorphic rock debris. In general, the increased reservoir porosity caused by the dissolution of mineral particles is not large, and approximately 5% of the reservoir porosity and permeability can be reconstructed (Marchand et al., 2002). Some minerals (e.g., carbonates) have mixed effects on the physical properties of rocks. Crystallization of early carbonate cements can reduce the size of primary pores; however, the dissolution of late carbonate cements during middle diagenesis can increase the porosity and permeability of a reservoir (Khan et al., 2020).

There is usually a positive correlation between the porosity and permeability of sandstone that formed under typical conditions, whereby permeability increases with increasing porosity (Zhou et al., 2011). However, there are very poor or negative correlations between porosity and permeability in some sandstones (i.e. permeability does not increase with increasing porosity) (Er et al., 2015). These rocks generally undergo uncommon processes of pore structure modification after typical sedimentation and diagenesis. These include contact with a hydrothermal fluid, strong dissolution, intense tectonism, and magmatism, which rapidly change the surrounding environment of rocks and make them more stable. The nature of the environment can change in a relatively short period of time, thus causing the physical parameter values to differ from those related to typical diagenesis (Ding et al., 2012; Mao et al., 2016; Liu et al., 2018). The sandstones in the third member of the Funing Formation have these special characteristics, with a poor correlation between sandstone porosity and permeability. The sandstone has a high porosity (23% on average) but a very low permeability (only $5 \times 10^{-3}\mu m^2$ on average), which is a very particular case in comparison to other low-permeability reservoirs. Most scholars believe that the decisive factors of a reservoir's physical properties are sedimentation and diagenesis, with late diagenetic alteration being the main reason for the poor correlation between porosity and permeability (Li et al., 2019b). We obtained a lot of useful information from a large number of studies as reference material in order to improve the reliability of our results (Zhang et al., 2018).

2 Geological setting

The Subei Basin is an onshore part of the Subei-South Yellow Sea Basin. It is bordered to the west by the Tanlu Fault and Lusu Uplift, and covers an area of approximately 35000 km^2. The interior of the basin can be divided into four secondary tectonic units from east to west: Dongtai Depression, Jianhu Uplift, Yanfu Depression, and Binhai Uplift (Shi et al., 2005; Gao, 2010). The Gaoyou Sag is located in the middle of the Dongtai Depression in the southern part of the Subei Basin. It is surrounded by the Lintong Uplift (south), Jianhu Uplift (north), Baiju Sag (east), and Lingtangqiao Uplift (west). Owing to differential uplift and subsidence, the southern part of the Gaoyou Sag is very steep, whereas the northern part is very gentle, thus resulting in an overall dustpan-like shape. From north to south, the tectonic units are divided into three parts: the northern slope zone, central deep-depression zone, and southern fault-terrace zone (Fig. 1).

The Gaoyou Sag is the main oil and gas bearing area in the Subei Basin, where the thickness of sedimentary rocks is considerable and the quality of source rocks is high. Therefore, various types of oil and gas reservoirs have formed with a high distribution density. The strata formed (from the bottom to the top) in the basin are the Taizhou, Funing, Dainan, Sanduo, and Yancheng formations. The main oil-bearing series are the Funing and Dainan formations. The target formation in this study is the Funing Formation, which was mainly formed by the interaction of sandstone and mudstone. The bottom of the Funing Formation is mainly composed of mudstone with a thickness of ~700–900 m. The sandstone content increases in the upper part, which has a thickness of 400–600 m and is the main oil-gas enrichment area (Cheng et al., 2019).

3 Methods

The research idea of this study is similar to that of fine reservoir characterization, which mainly includes the study of sedimentary genesis, distribution law, diagenesis process, and pore structure characteristics of sandstone. However, differing from the conventional process, the influence of sedimentation and diagenesis on the physical properties of sandstone was analyzed more systematically and deeply. The basic characteristics of high porosity and

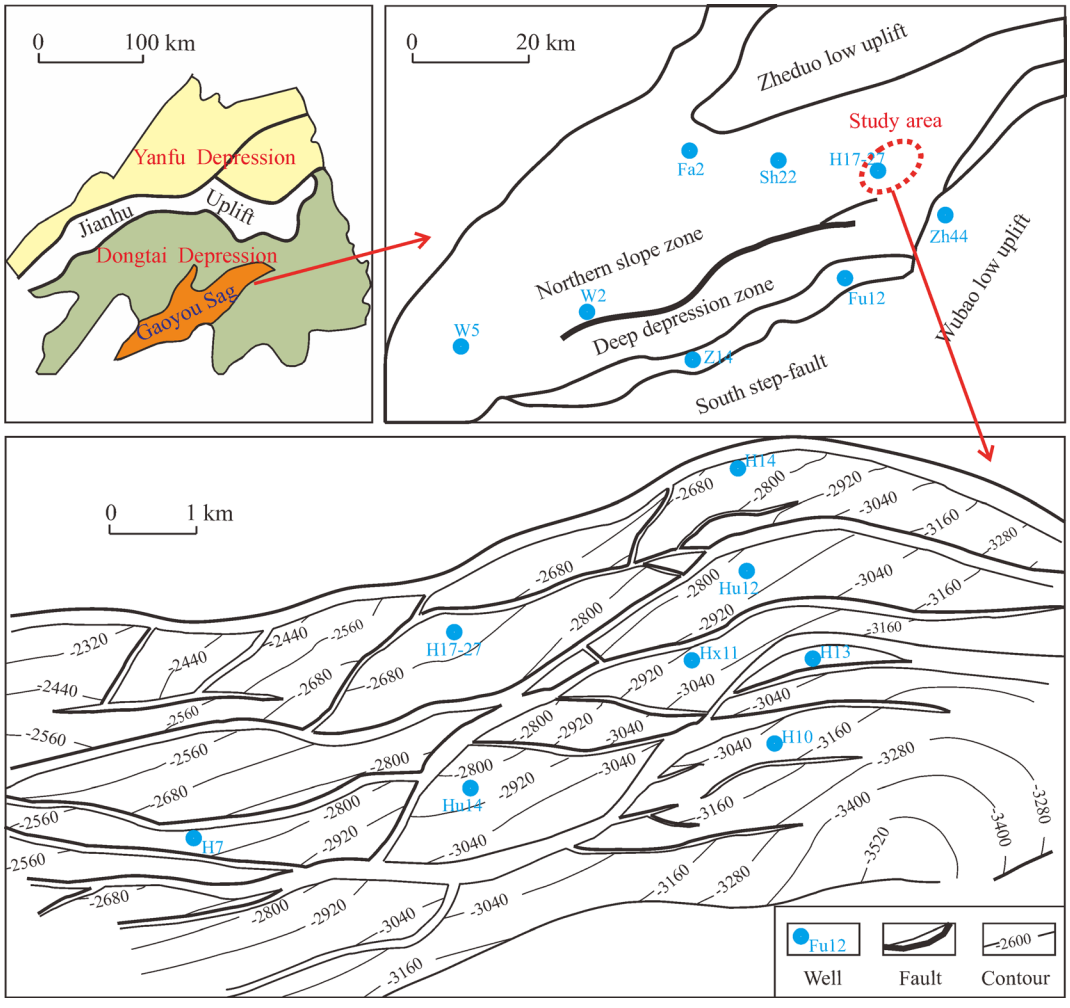

Fig. 1 Location map of the study area.

low permeability were determined, and the causes of abnormal physical properties were clarified (Fig. 2).

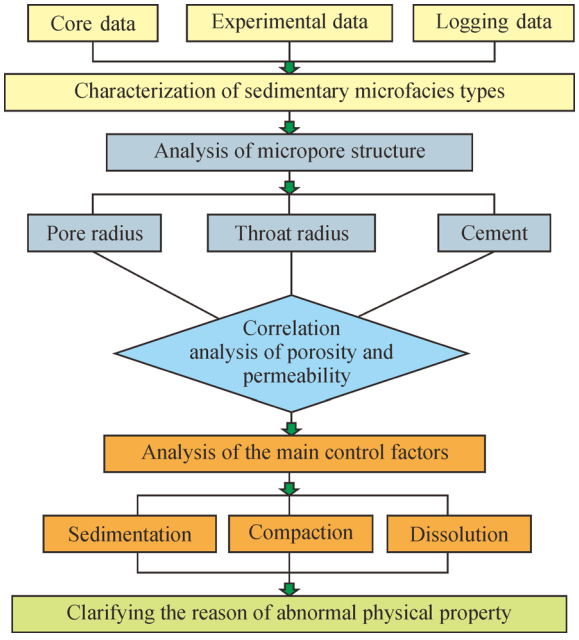

Fig. 2 Schematic of the research ideas and process.

1) Sedimentary facies

The foundation of research into sedimentary facies is the abundant core data and experimental data that are used to study the material composition, sorting characteristics, sedimentary background, and sedimentary environment of rocks (Zhang et al., 2019). A single-well facies model was established in the present study to determine the relationships between the changes in the physical properties and sedimentary microfacies.

2) Pore structure analysis

Based on microscopic experimental data, the geometry, size, distribution, and interconnection of pores and throats were analyzed. The correlations between the pore structure, reservoir capacity, and seepage capacity (porosity and permeability) of reservoir rocks were then determined (Li et al., 2019a).

3) Analysis of factors influencing porosity and permeability

Based on the analysis of a considerable amount of rock micro-experimental data, the pore structure characteristics of the reservoir were systematically characterized, and the distribution law as well as the sizes of pores and throats were clarified. The genesis and secondary change process of the pores and throats were analyzed, and the main reason for the high porosity and low permeability of sandstone in the study area was determined (Li et al., 2016).

4 Results

4.1 Petrological characteristics and sedimentary facies

The E_1f_3 strata were observed to be dominantly composed of black or gray-black mudstone (content of ~60%). This coloring indicates that the sedimentary area is far from the source area. The sandstone within the core was mainly fine-grained siltstone (content of 41.7%; Fig. 3(a)), which was followed by silty mudstone and a small amount of fine to medium sandstone. The fine-grained characteristic and high shale content of this sandstone are consistent with a sedimentary environment. The sandstone also presented a good structural maturity, as reflected by the good sorting, high grinding roundness, and linear points of contact between the particles. In addition, the quartz content was very high, whereas the feldspar and detritus contents were relatively low (Fig. 3(a)). The average composition maturity index of the rock was found to be 1.44. These characteristics indicate the long-distance transport of the particles.

The structural characteristics of a sedimentary rock can be identified directly from drilling core data; thus, the sedimentary environment and facies of the formation can be inferred. The main sedimentary structures observed from the core profile revealed the characteristics of delta front sedimentary subfacies, which contained low-angle cross bedding, wavy bedding, sandy bedding, and flattened bedding. The contact interface between sandstone and mudstone was essentially flat, and no obvious channel scouring structure was observed. This indicates that the channel was not the dominant factor of the sedimentation process. Mudstone was usually deposited between distributary channels, which had experienced some biological disturbance (Fig. 3(b)).

Single-well facies analysis can be used to detail the characterization of drilling core data, which is an aggregate of lithofacies and sedimentary facies. A series of characteristics, including the rock composition, internal structure, sedimentary structure, bedding cycle, grain size change, color change, and palaeontology, can be described in a single-well facies profile. Figure 4 presents the single-well facies characteristics of well H17-27. This indicates that the subfacies type in the study area is that of a river-controlled delta front with four different microfacies: distributary channel, mouth bar, sand sheet, and interdistributary microfacies. Among them, the mouth bar microfacies was found to dominate, and was mainly composed of fine sandstone and siltstone. This sedimentary process took place under the paleogeographic background of a gently sloping basin influenced by weakened tectonic subsidence and an increased source supply (Li et al., 2012).

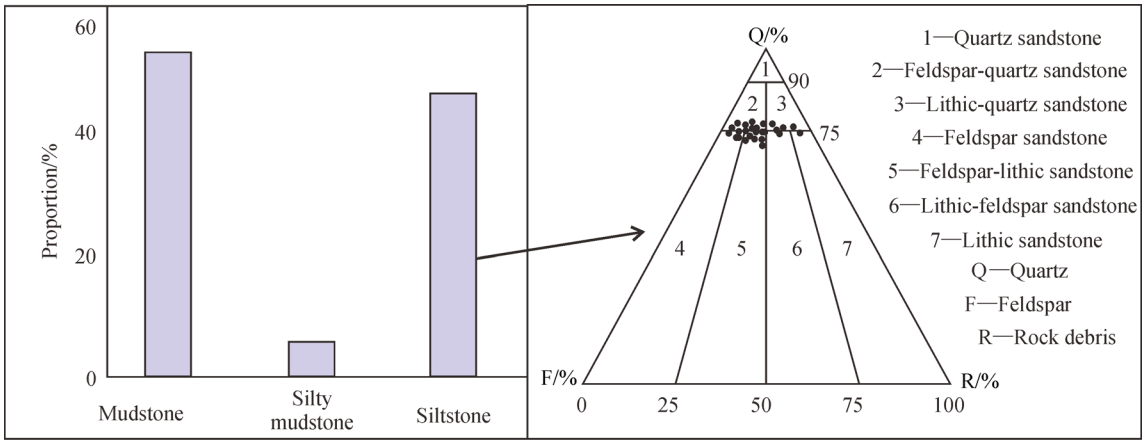

(a) Lithological statistics

(b) Characteristics of sedimentary structures

Fig. 3 Lithological statistics and characteristics of a sedimentary core from the study area.

4.2 Pore and throat sizes and their statistical regularity

The average porosity of the sandstone samples was 18.95% and the average permeability was 5.46×10^{-3} μm^2 (Table 1). The permeability of 74.3% of the samples ranged from 2×10^{-3} μm^2 to 8×10^{-3} μm^2. The carbonate rock content of the sandstone was moderate, whereas the shale content was high. These characteristics affect the development of pores and throats.

1) Pore and throat sizes

The sandstone samples contained intergranular pores, intragranular pores, dissolution pores, and matrix micropores. Dissolution pores were the most important pore type and were categorized into two types: dissolution intragranular pores (Fig. 5(a)) and dissolution intergranular pores (Fig. 5(b)). Intragranular pores were mainly granular pores formed by dissolution feldspar, with local intergranular pores and microcracks. Intergranular pores were poorly connected and were mainly reduced residual pores controlled by compaction (Figs. 5(c) and 5(d)). The primary pore assemblage of the sandstone samples was found to be dissolved pores-intergranular pores. The throats in part of the cross section had primarily formed by shrinkage, and sheet or bent sheet throats were also observed. Overall, the throats were small, well distributed, and uneven. The pore connectivity was poor and there was no throat connection between some large pores; thus, many pores were observed to be isolated.

The pore throats of clastic rock represent the channels connecting adjacent pores. There are various types of

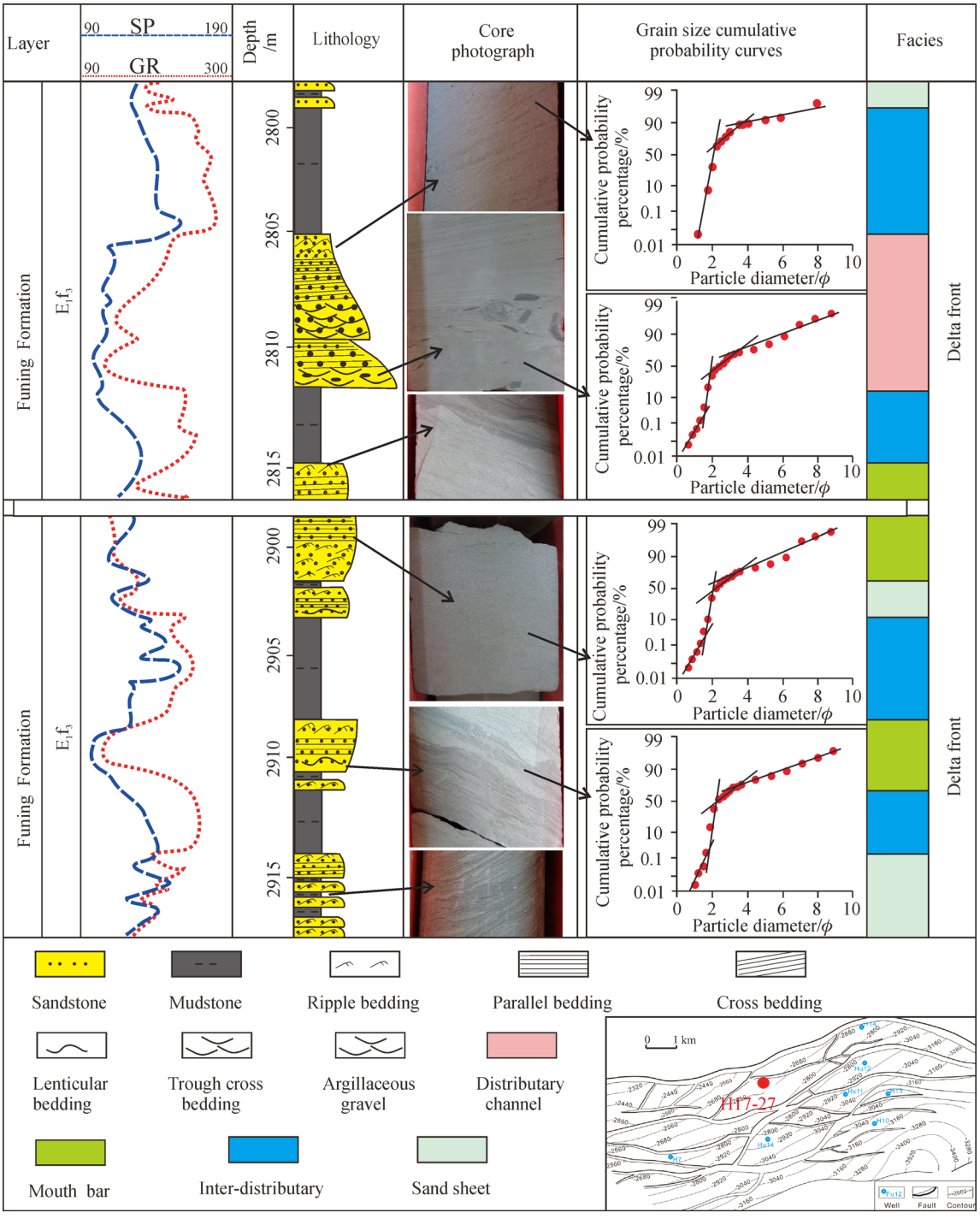

Fig. 4 Single-well facies of H17-27.

Table 1 Physical parameters of the sandstone samples

Number of samples	Porosity/%		Permeability/(10^{-3}μm^2)		Argillaceous content/%		Carbonate content/%	
	Range	Average	Range	Average	Range	Average	Range	Average
39	4–25	18.95	0.03–17	5.46	4.7–15.39	8.5	0.19–21.6	3.8

throats, including pore shrinkage throat, sheet throat, bending sheet throat, and tube-shaped throat, which are used indicate pore connectivity (Wang et al., 2019). Obviously, the size, distribution, and geometry of throats are the main factors affecting the percolation characteristics of reservoir rocks. The pore throat type of sandstone in a reservoir differs depending on the contact between rock particles, the size and shape of sand particles, and the type of cementation (Guo et al., 2020). The clastic grains of the sandstone samples were mostly inlaid with each other, thus leaving a relatively small space for the throats. The pore throats of the sandstone samples were mainly composed of sheet throats and bending sheet throats. The pores were very small and the throats were very fine; hence, they could become blocked easily. According to the morphology and connectivity of the throats, they were divided into four different classes as follows. Class I: very good connectivity and very regular shape; class II: good connectivity and regular shape; class III: moderate connectivity and irregular shape; class IV: poor connectivity and extremely irregular shape (Fig. 5(f)).

2) Pore and throat statistical regularity

The absolute dimensions of each pore and throat can be measured by constant-rate mercury injection for statistical analysis of the distribution rule and proportion of each type of pore and groove (Gao et al., 2011; Clarkson et al., 2013). The frequency chart of the pore distribution of the sandstone samples shows that the average pore radius was 150 μm, which indicates intermediate porosity, although the proportion of pores with radii >200 μm was also relatively large (Fig. 6(a)). However, the average throat radius was only 15 μm, and the average pore/throat ratio was 10; therefore, the throats were considered to be micro-throats (Fig. 6(b)). This finding indicates that one of the physical parameters of reservoir porosity or permeability was strongly modified during the later diagenesis stage. In addition, there was also a strong correlation between porosity and the maximum mercury saturation

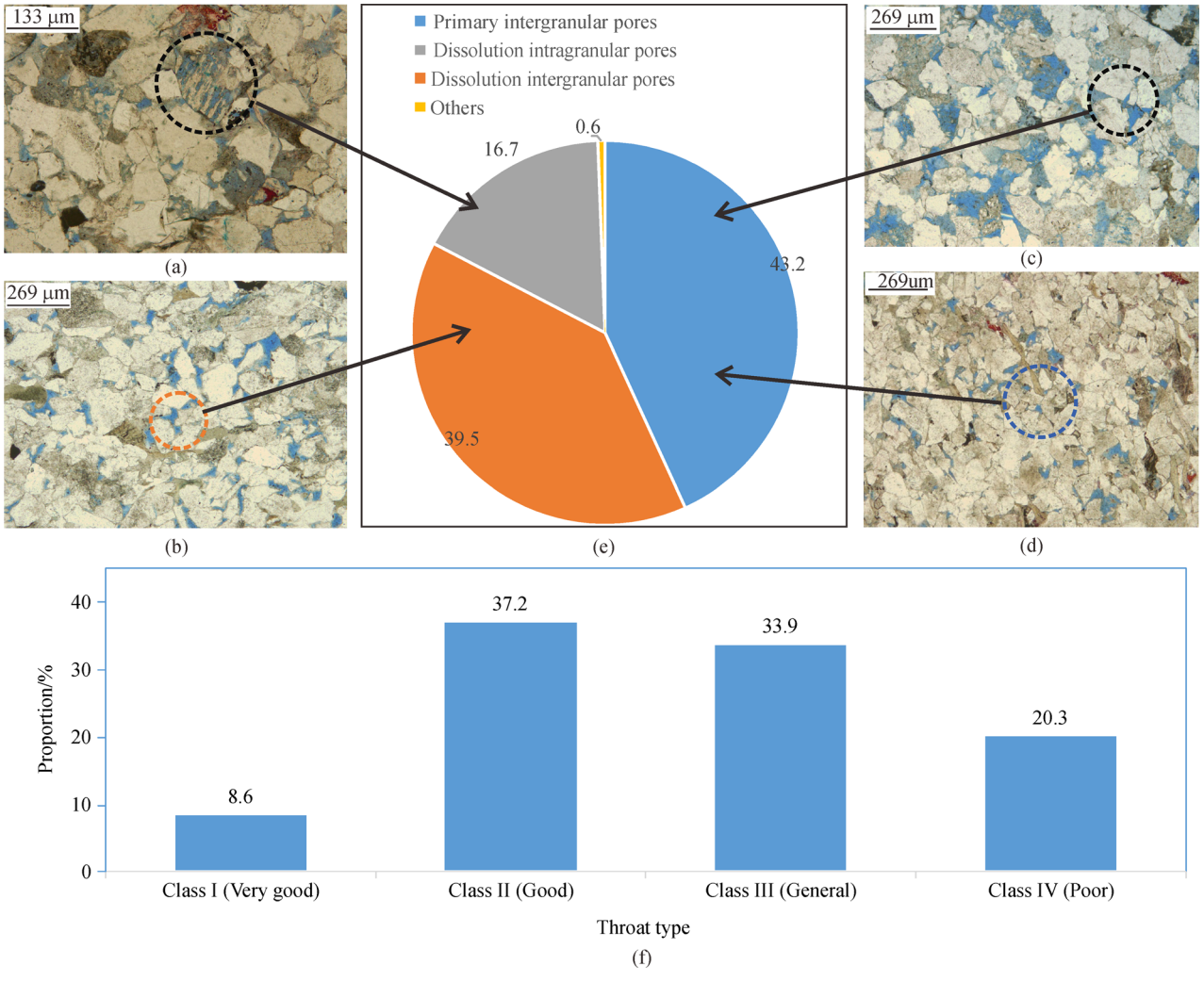

Fig. 5 Types and characteristics of pores and throats. (a): Hx28, 3260.37 m (general); (b): Hx17, 2910.65 m (good); (c): H26-5, 2915.43 m (very good); (d): Hx38, 2725.45 m (poor); (f): throat characteristics and statistics of sandstone.

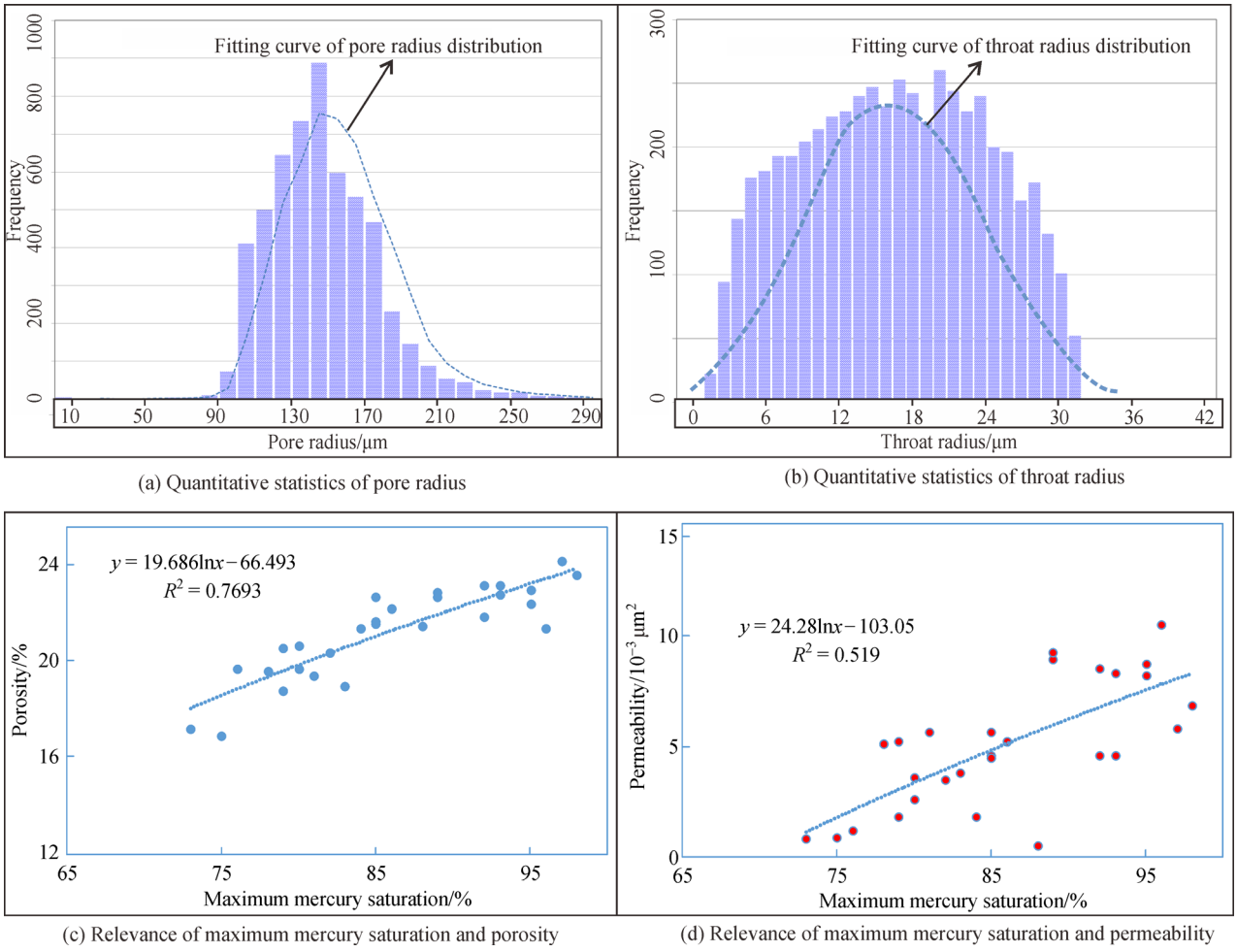

Fig. 6 Quantitative statistics for the constant-rate mercury injection experiment data.

determined in the mercury injection experiments. Hence, although the physical conditions of the rocks were poor, their overall porosity was high provided there were many types of post-reconstruction pores. However, there was a poor correlation between permeability and the maximum mercury saturation, which indicates that the former was less affected by later diagenesis and that the original throats were preserved (Figs. 6(c) and 6(d)).

4.3 Analysis of uncorrelated physical properties

The pore and throat distribution ranges of the sandstone samples indicate an intermediate porosity and ultralow permeability, thus reflecting the abnormal phenomenon of the correlation between physical parameters. Many related studies have revealed that a very poor correlation between physical parameters can be attributed to the influencing processes of sandstone formation and later transformation (Bloch and Helmold, 1995).

To ascertain the reason for the poor correlation between reservoir porosity and permeability in the study area, three similar reservoirs in other basins were selected for comparative analysis: the Nenjiang Formation reservoir in the Songliao Basin, the Shahejie Formation reservoir in the Bohai Bay Basin, and the Yanchang Formation reservoir in the Ordos Basin (Wang et al., 2015). These reservoir sedimentary facies are all river delta facies, and the composition, grain size, and structure of the corresponding sandstones are similar; thus, it is possible to determine any correlations between them. The correlation between reservoir porosity and permeability in the study area was poor, which is clearly different from the fairly typical correlations in the other three reservoirs (Fig. 7) with a high porosity and extremely low permeability. According to the previous selection criteria, the influence of sedimentation could be excluded; hence, diagenesis was considered to be the main reason for this difference (Tang et al., 2013).

5 Discussion

We infer that the abnormal variation of porosity and permeability of reservoir sandstone in the study area is mainly caused by a difference in the diagenesis stage that occurred after sedimentation. The E_1f_3 sandstone burial

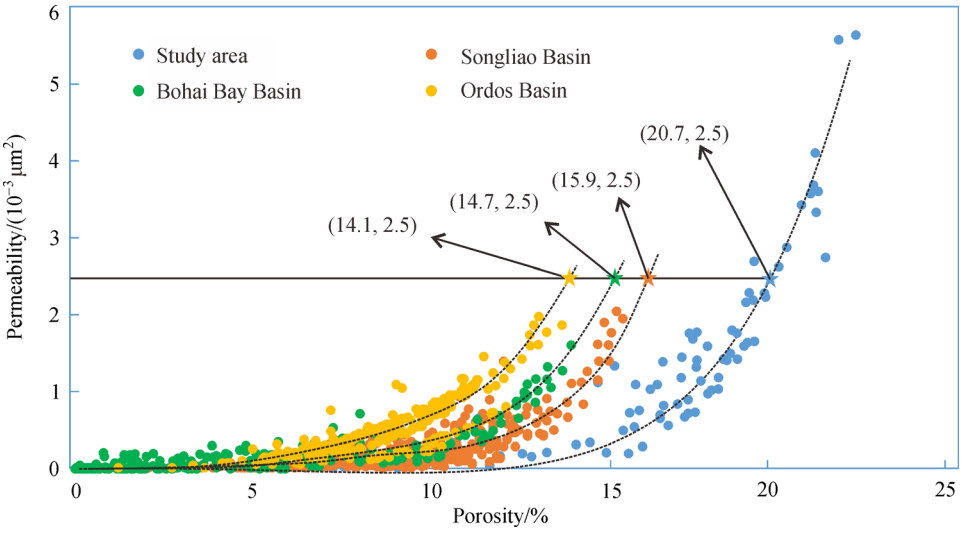

Fig. 7 Physical parameter correlations of sandstones from different reservoirs.

depth in the study area is more than 2800 m, which should be classified as tight sandstone characterized by ultra-low porosity and permeability. However, the porosity of this sandstone is very abnormal and of a medium level, which indicates that it has been significantly modified from its initial value by later diagenesis. Consequently, we can analyze the diagenesis effect on sandstone porosity to explore which stage and which process changed the original porosity (Wang et al., 2018a). Sneider diagram suggests that the initial sandstone porosity was approximately 40%. During diagenesis, sandstone underwent large pore changes during three stages (Zhang et al., 2010). The first stage involved initial compaction and cementation, with compaction dominating; these destructive diagenetic processes reduced the primary porosity. In addition, an increased quartz content and calcite cementation during the early stage of diagenesis also reduced the primary porosity, although the effect was weaker than that of compaction. The second stage involved dissolution that created pores. The dissolution of particles and fillings is the main diagenetic process by which secondary pore zones are formed. The third stage involved later cementation; for example, filling with clay minerals such as illite, kaolinite, and chlorite (Li et al., 2019a). In addition, the precipitation of pyrite and other minerals also affected the reservoir pore characteristics to some degree. Although this was a destructive diagenetic process, its influence was smaller than that of the initial compaction and cementation (Fig. 8).

5.1 Degree of pore destruction by compaction

Continuous compaction causes an irreversible loss of pore space in sandstone, with porosity decreasing linearly with increased depth. According to the regression formula, the relationship between the decreased rock porosity and increased depth can be expressed by Eq. (1):

$$\Phi = 40.35 - 0.0079H, \quad (1)$$

where Φ is porosity and H is formation depth.

According to Eq. (1), rock porosity decreases by ~8% for every 1000 m of formation depth.

In addition, under the same compaction conditions, the decrease in porosity is related to the type of rock. In general, the pore skeleton of rocks with a good particle sorting, large particles, and large porosity (e.g., pure fine sandstone and medium sandstone) is greatly altered by compression. The porosity of rocks with small grains and dense pores, or with a high cement content, is less affected by compaction. Figure 9 presents a statistical map of the variation in porosity for different types of sandstone with increasing depth in the study area. The map clearly shows that with increasing burial depth, the porosity of the rocks tends to decrease gradually, although sandstones with less cementation clearly exhibit a more rapid decrease than those with more cementation. Rocks with higher calcareous and argillaceous contents are less affected by compaction. Sandstone cements have relatively high clay mineral and carbonate contents. Therefore, under compaction conditions at approximately 3000 m, the porosity of the cements decrease by approximately 20%, which is slightly lower than the average reduction.

5.2 Destruction of pores by cementation

1) Effect of clay minerals

As the formation burial depth increases, the pressure and temperature also increase. In this process, the interlayer water is discharged and clay minerals recrystallize (Ahlberg et al., 2003). Affected by provenance and sedimentation, the content and type of clay minerals have complex and variable relationships with burial depth. The main types of clay minerals in this study included an

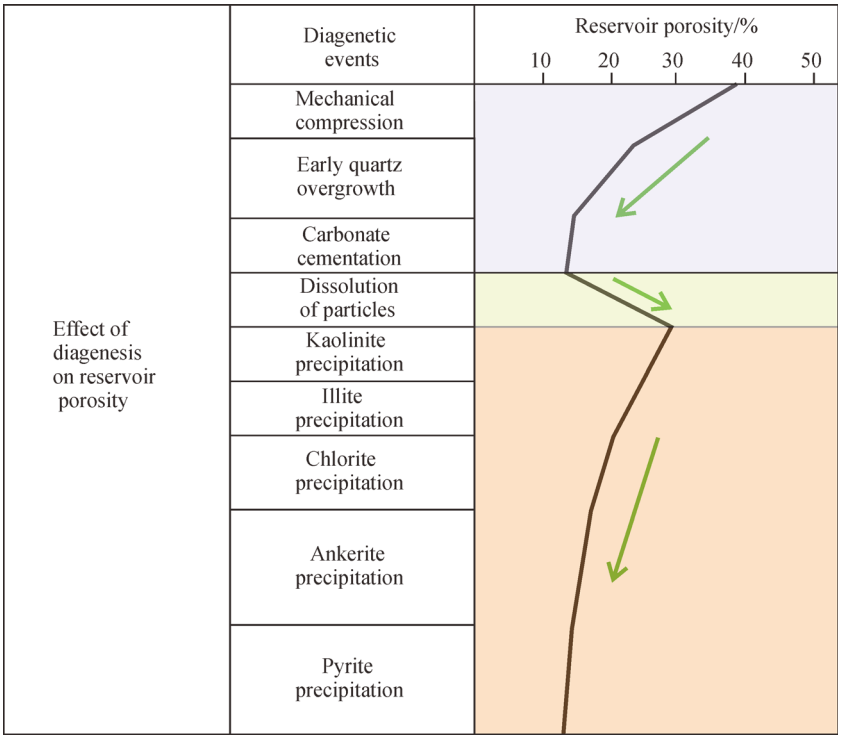

Fig. 8 Effect of reservoir diagenetic events on porosity.

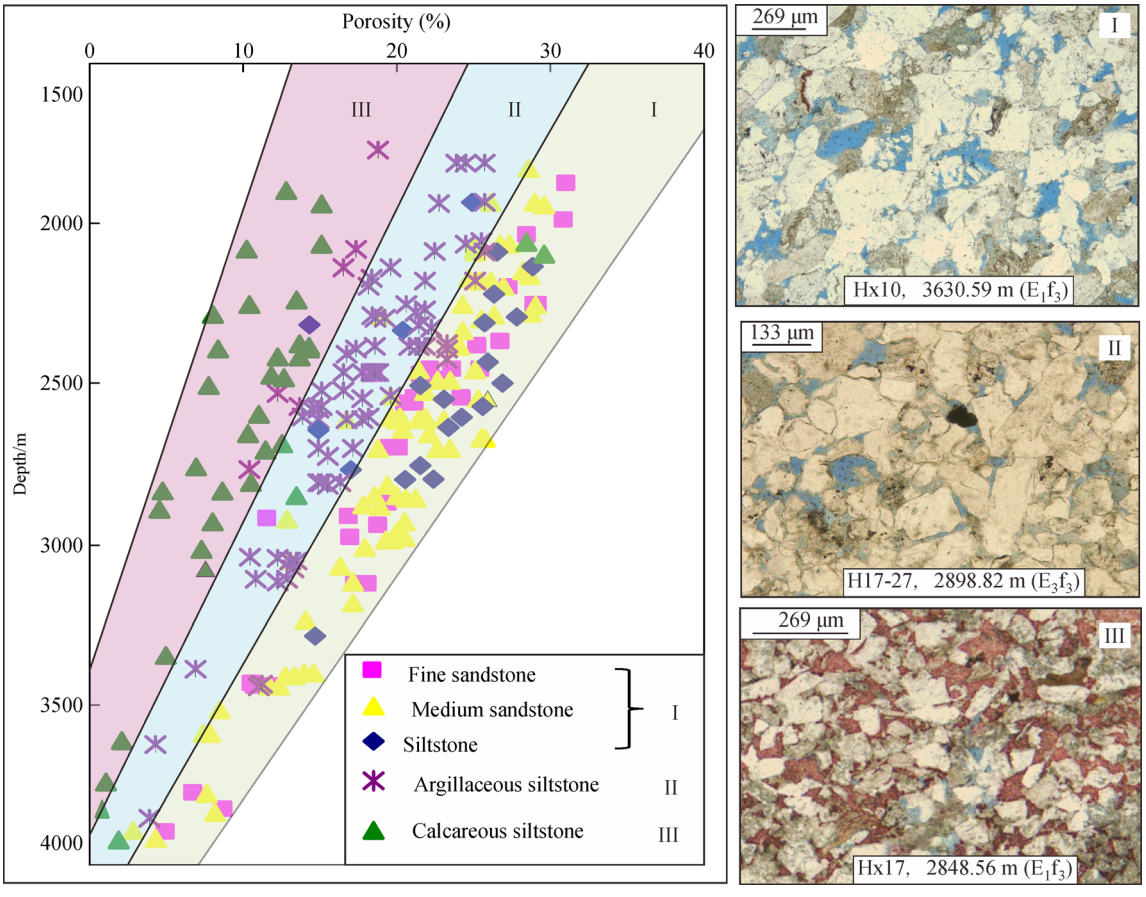

Fig. 9 Porosity variation rate with depth for different types of sandstone.

illite-montmorillonite mixed layer (I-M mixed layer), illite, kaolinite, and chlorite. Among them, the relative content of the I-M mixed layer was approximately 35%, which was the dominant component. With increasing depth, the montmorillonite in the I-M mixed layer transformed to illite and then chlorite. Therefore, the montmorillonite content was negatively correlated with depth, although this was not obvious (Fig. 10(a)). With increasing depth, the proportion of illite usually increases; however, this was not the case for the sandstone in the study area (average content of 25%), which was not greatly affected by the conversion of deep montmorillonite. The main reason for the high illite content in shallow areas is that kaolinite forms after the dissolution of feldspar and debris transforms into illite, thus resulting in a high illite content throughout the vertical profile (Fig. 10(b)). This is consistent with the development of dissolution in this area. The kaolinite and chlorite contents decreased with increasing burial depth, which relates to mineral dissolution in the target interval (Figs. 10(c) and 10(d)). According to the clay mineral content change rule, mineral transformation due to temperature and pressure plays a relatively small role, whereas mineral transformation by dissolution is dominant.

2) Effect of carbonate cements on the physical properties of rocks

The content of carbonate cement in the sandstone pores and throats was also relatively high (8% on average). However, the dissolution of carbonate minerals in the pores was difficult to observe, possibly as there was only a very small amount of dissolution. This resulted in an obvious decrease in rock porosity with an increase in the carbonate mineral content (Fig. 11(a)). However, the correlation between the permeability and carbonate mineral content was poor. This indicates that the degree of dissolution of carbonate minerals in the pores and throats was very low during the later diagenesis stage (dissolution); hence, the dissolution of the carbonate cement contributed only slightly to the permeability change (Fig. 11(b)). The correlation map of the carbonate content and reservoir physical properties shows that the physical properties (especially the porosity) were degraded as the carbonate content increased.

3) Cement effects analysis

If the cement in the pores is removed completely, the ratio of pores to the total volume of sandstone can be called the minus-cement porosity (Houseknecht, 1984; Lei et al., 2010). This metric can be used to characterize the effects of

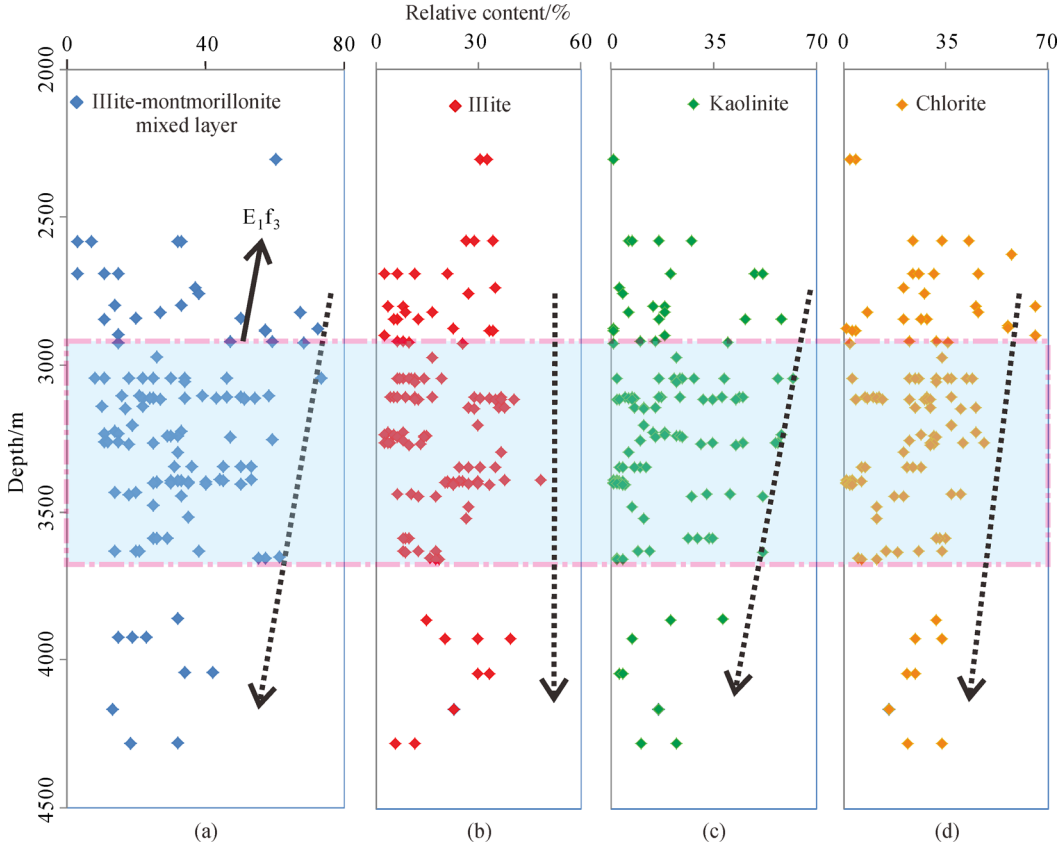

Fig. 10 Variation in clay mineral contents with depth.

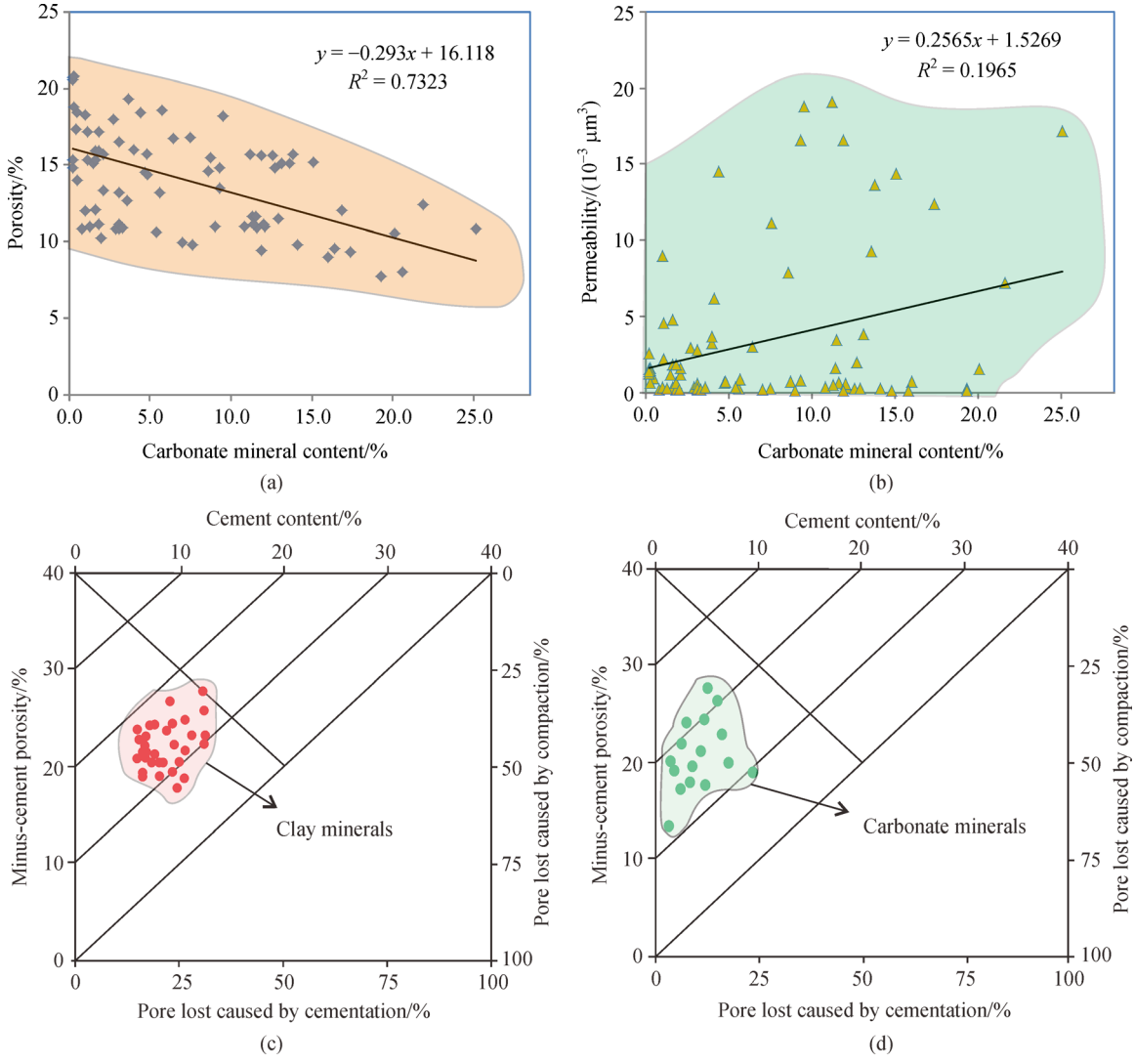

Fig. 11 Relationship between physical properties and cement content. (a) relationship between porosity and cement content; (b) relationship between permeability and cement content; (c) relationship between minus-cement porosity and pore loss due to carbonate cementation; (d) relationship between minus-cement porosity and pore loss due to carbonate cementation.

different types of cementation on the pores in the rock. The sandstone minus-cement porosity projection can be presented by using 1) the cement content obtained from the experiment, and 2) the porosity value after removing the cement. This can be used to judge the degree of influence of compaction and cementation of sandstone pores on the physical parameters of the rock. The minus-cement porosity projection for the study area suggests that the physical parameters were affected mainly by compaction, whereas the effect of cementation was not obvious. Therefore, it can be speculated that the strong compaction of strata might be the main factor that significantly decreased the rock porosity and permeability (Figs. 11(c) and 10(d)).

5.3 Constructive effect of dissolution on pores

The dissolution of rock skeleton particles and diagenetic minerals in a fluid medium often occurs during diagenesis; it is a constructive process that can produce secondary porosity and improve the physical properties of a reservoir (Zou et al., 2015). Dissolution of sandstone particles or cements can produce high-quality reservoirs, such as ‘sweet spots’ in tight sandstone reservoirs (Lai et al., 2020). Organic acids are usually the main cause of the formation of dissolution pores in sandstone (Mosavat et al., 2019). Dissolution is very common in sandstone reservoirs, whereby feldspar and carbonate minerals are mainly dissolved. In addition, debris dissolution phenomena are also observed, but filling dissolution is not obvious (Wang et al., 2014). The dissolution of feldspar particles is mainly due to organic acids. The edges of the dissolved feldspar particles were observed to be generally bay-like, and the strongly dissolved feldspar particle were either debris-like or formed intragranular dissolved pores (Figs. 12(a), 12(b) and 12(c)). Dissolution of carbonate minerals, mostly

minor calcite dissolution, was also observed under a microscope and scanning electron microscope (Figs. 12(d), 12(e) and 12(f)). The dissolution degree of carbonate cements was relatively low and the contribution to secondary pores was relatively small. Debris dissolution was not obvious in the studied sandstone and the degree of dissolution was low. The main dissolution types were partial dissolution of debris and occasional dissolution of biological debris (Figs. 12(g), 12(h) and 12(i)). Debris with a higher degree of dissolution could also form larger intragranular pores.

The thin section observations and statistical results revealed that the dissolution of feldspar was most common in the sandstone samples, accounting for 69% of the total dissolution pores. The proportions of pores formed by the dissolution of carbonate minerals and soft sediment particles (rock debris) were similar (14% and 13%, respectively). The dissolution proportion of other particles (clay minerals) was relatively small (4%); Fig. 13.

Dissolution is the dominant factor altering the porosity of sandstone, and many types of dissolution can occur in rocks. There is ample evidence of the degree to which dissolution can alter the pore structure. The dissolution of sandstone in the study area was found to be very strong.

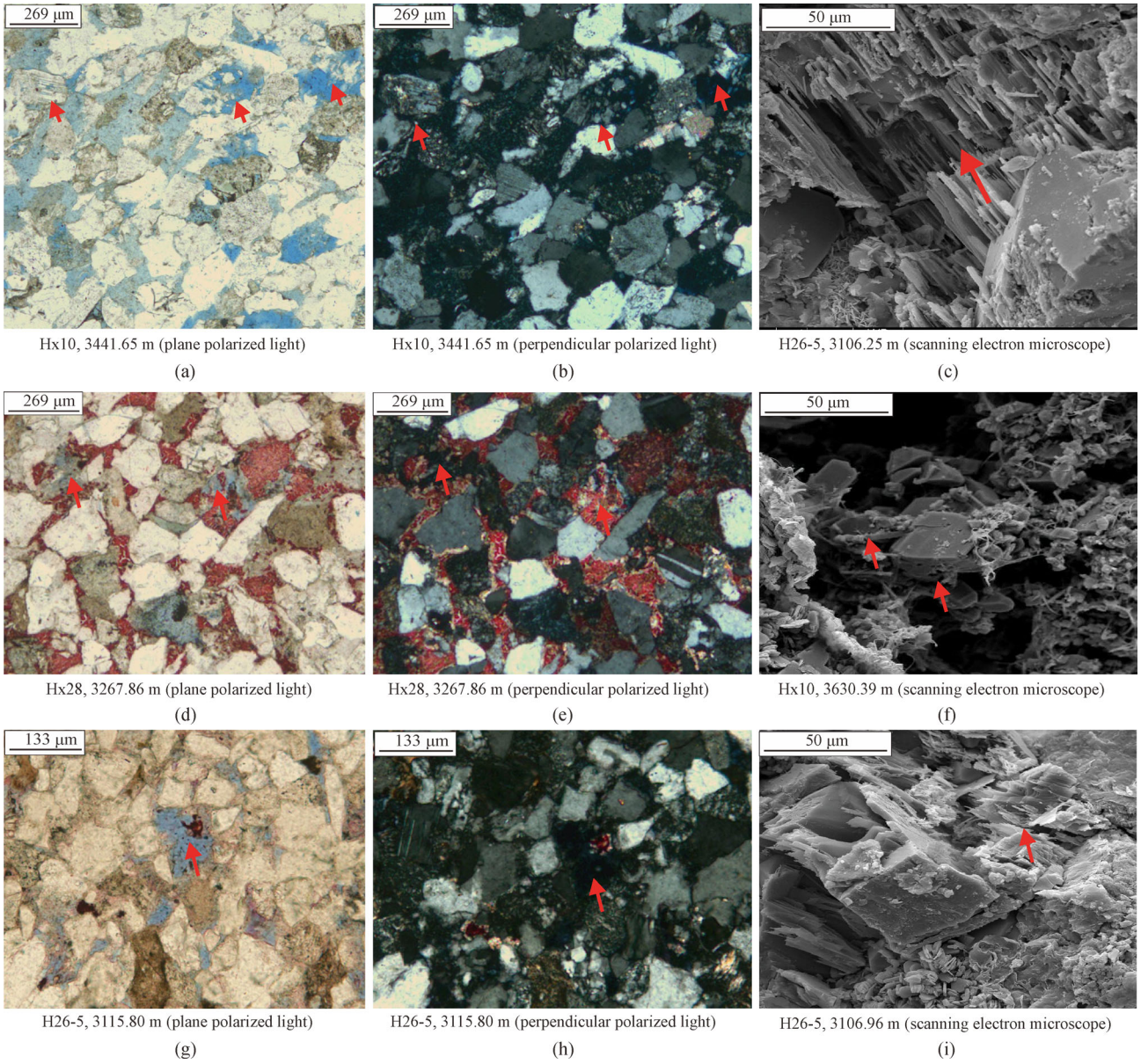

Fig. 12 Dissolution phenomena in sandstone. (a) feldspar observed by a monopolar microscope; (b) feldspar observed by orthogonal polarizing microscope; (c) feldspar observed by a SEM; (d) calcite observed by a monopolar microscope; (e) calcite observed by an orthogonal polarizing microscope; (f) calcite observed by a SEM; (g) debris observed by a monopolar microscope; (h) debris observed by an orthogonal polarizing microscope; (i) debris observed by a SEM.

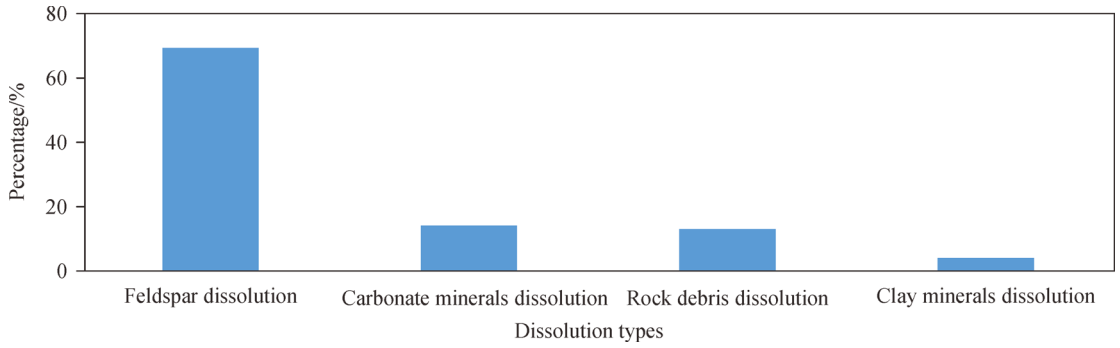

Fig. 13 Different dissolution types of clastic particles.

Feldspar accounted for the vast majority of the eroded clastic particles, the total or partial dissolution of feldspar has mainly promoted an increased in the number of pores. The degree of dissolution of the carbonate minerals and clay minerals filling the pores and throats was very low; the pore connectivity was not effectively improved, thus leading to the high porosity-low permeability phenomenon of this sandstone. Therefore, the correlation between porosity and permeability can reflect the late diagenesis of rocks in some ways. The average reservoir porosity was approximately 19%, thus indicating an intermediate porosity; however, the pore sorting was not good, and the pore types were complex and diverse. Intergranular and intragranular dissolution pores collectively accounted for ~56% of the total pore space, whereas primary pores comprised only ~43%. A quantitative pore evaluation by the constant-rate mercury injection experiment gave the same result. Two obvious peaks were observed in the pore distribution diagram, with the peak on the left representing the primary intergranular pores and the peak on the right representing the dissolution pores (Fig. 14(a)). Their average values were 100 μm and 180 μm, respectively; i.e., the later was nearly twice that of the former. The main reason for the pore size increase may have been the presence of a large number of dissolution pores with a diameter that was almost twice that of the original pores. Moreover, the total porosity was approximately 1.5 times that of the original porosity.

The above analysis indicates that the sandstone porosity has been obviously affected by later dissolution. We evaluated 1) whether dissolution occurs in the throats connecting the pores, and 2) the role of the throats formed by dissolution in the entire connecting system by using the results of the constant-rate mercury injection experiment. Figure 14(b) presents a statistical chart that quantitative describes the distribution characteristics of the sandstone throats. This shows that the throat diameter ranged widely (1–45 μm) and that the average value was very small (~15 μm), thus indicating that dissolution of the filling materials in the pores and throats was selective and not uniform/regular (Wang et al., 2018b). Moreover, the proportion of cement dissolution was not dominant or high. The dissolution pores in the grains accounted for 40% of the total pores, whereas the dissolution pores between the grains accounted for only approximately 16%. Therefore, it can be inferred that dissolution only increases the porosity of rocks in the study area, but does not improve the connectivity between them; thus, the reservoir porosity is relatively high, but the permeability is very low.

6 Conclusions

1) The sedimentary facies of the E_1f_3 in the study area is river delta, the microfacies include distributary channels, mouth bars, sand sheets, and interdistributary, where mouth bar is the dominate one. Fine grain size and high argillaceous content are the main reasons for the small primary pores and poor throat connectivity. However, a high feldspar content in the sediments promotes the occurrence of later dissolution, which is a prerequisite for the generation of a large number of secondary pores.

2) Compaction and cementation are the main destructive diagenetic processes, which decrease the primary porosity of sandstone by 60%. However, the secondary porosity of sandstone dominates due to the strong dissolution of clastic particles (feldspar, carbonate mineral, and rock debris) during the later stage of diagenesis. Consequently, the porosity of the studied sandstone is obviously higher than that of typical low-permeability sandstones.

3) Feldspar particles in the studied sandstone are the main object of dissolution transformation, although no large-scale dissolution was observed for the carbonate minerals filling pores and throats. Therefore, dissolution has increased the porosity of rock without significantly improving the connectivity between the pores. This is essentially the reason for the high porosity but very low permeability of sandstone in the study area.

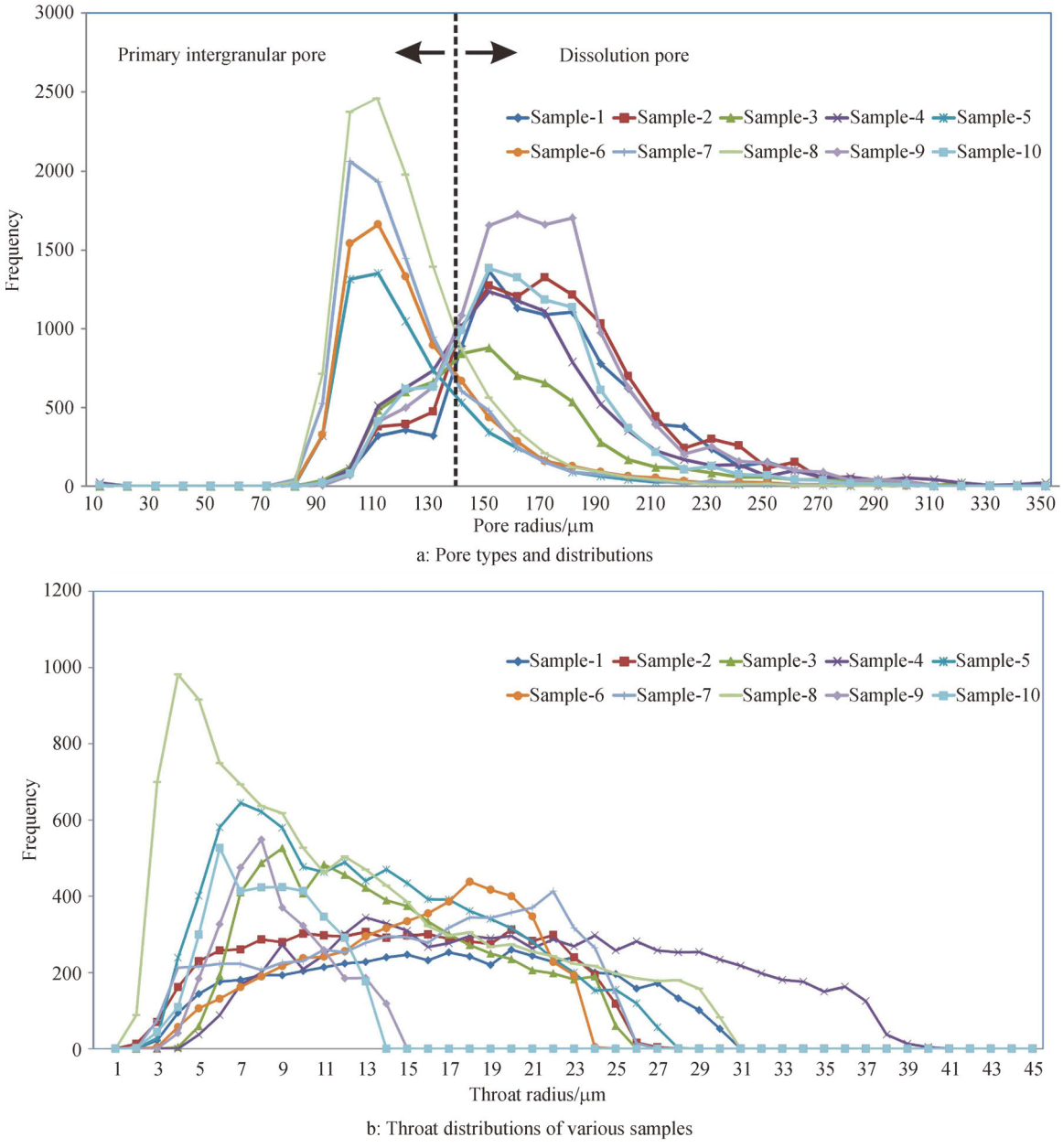

Fig. 14 Reservoir pore and throat distributions of various samples from the study area.

References

Ahlberg A, Olsson I, 0Simkevicius P (2003). Triassic-Jurassic weathering and clay mineral dispersal in basement areas and sedimentary basins of southern Sweden. Sediment Geol, 161(1–2): 15–29

Aoyagi K, Kazama T (1980). Transformational changes of clay minerals, zeolites and silica minerals during diagenesis. Sedimentology, 27(2): 179–188

Arostegui J, Sangüesa F, Nieto F, Uriarte J A (2006). Thermal models and clay diagenesis in the Tertiary-Cretaceous sediments of the Alava block (Basque-Cantabrian Basin, Spain). Clay Miner, 41(4): 791–809

Ballas G, Garziglia S, Sultan N, Pelleter E, Toucanne S, Marsset T, Riboulot V, Ker S (2018). Influence of early diagenesis on geotechnical properties of clay sediments (Romania, Black Sea). Eng Geol, 240: 175–188

Bloch S, Helmold K (1995). Approaches to predicting reservoir quality in sandstones. AAPG Bull, 79: 97–115

Cheng Q, Zhang M, Li H (2019). Anomalous distribution of steranes in deep lacustrine facies low maturity-maturity source rocks and oil of Funing formation in Subei Basin. J Petrol Sci Eng, 181: 106190

Clarkson C, Solano N, Bustin R M, Bustin A M M, Chalmers G R L, He L, Melnichenko Y B, Radliński A P, Blach T P (2013). Pore structure characterization of North American shale gas reservoirs; using USANS/SANS, gas adsorption, and mercury intrusion. Fuel, 103: 606–616

Dillinger A, Ricard L P, Huddlestone-Holmes C, Esteban L (2014). Impact of diagenesis on reservoir quality in a sedimentary geothermal play: a case study in the Cooper Basin, South Australia. Basin Res, 28: 1–10

Ding S, Zhong S, Gao G, Liu Q, Sun X Q (2012). Quantitative evaluation of low permeability reservoir diagenetic facies by combining logging and geology. Journal of Southwest Petroleum University, 34: 83–87 (in Chinese)

Er C, Zhao J, Bai Y, Wu W T, Zhang J (2015). Features of tight sandstone reservoir and origin of tightness: an example from Chang-7 Member, Triassic Yanchang Formation in Chenghao area, Ordos Basin. Acta Geologica Sinica-English Edition 89: 25–26

Gao H, Xie W, Yang J P, Sun W (2011). Pore throat characteristics of extra-ultra low permeability sandstone reservoir based on constant-rate mercury penetration technique. Petroleum Geology & Experiment, 33: 206–211 + 214 (in Chinese)

Gao L (2010). Sedimentary facies and evolution of Paleogene Dainan Formation in Gaoyou Sag, Subei Basin. Acta Sedimentologica Sinica, 28: 706–716 (in Chinese)

Guo R, Xie Q, Qu F, Chu M, Li S, Ma D, Ma X (2020). Fractal characteristics of pore-throat structure and permeability estimation of tight sandstone reservoirs: a case study of Chang 7 of the Upper Triassic Yanchang Formation in Longdong area, Ordos Basin, China. J Petrol Sci Eng, 184: 106555

Glombitza C, Mangelsdorf K, Horsfield B (2016). Differences in bitumen and kerogen-bound fatty acid fractions during diagenesis and early catagenesis in a maturity series of New Zealand coals. Int J Coal Geol, 153: 28–36

Herlinger R, Zambonato E, De R, Luiz F (2017). Influence of diagenesis on the quality of lower cretaceous pre-salt lacustrine carbonate reservoirs from northern Campos Basin, Offshore Brazil. J Sediment Res, 87(12): 1285–1313

Hood A, Planavsky N, Wallace M W, Wang X (2018). The effects of diagenesis on geochemical paleoredox proxies in sedimentary carbonates. Geochim Cosmochim Acta, 232: 265–287

Houseknecht D, David W H (1984). Influence of grain size and temperature on intergranular pressure solution, quartz cementation, and porosity in a quartzose sandstone. J Sediment Res, 54: 348–361

Khan Z, Sachan H, Ahmad A, Ghaznavi A A (2020). Microfacies, diagenesis, and stable isotope analysis of the Jurassic Jumara Dome carbonates, Kachchh, Western India: implications for depositional environments and reservoir quality. Geol J, 55(1): 1041–1061

Lai J, Fan X, Liu B, Pang X, Zhu S, Xie W, Wang G (2020). Qualitative and quantitative prediction of diagenetic facies via well logs. Mar Pet Geol, 120: 104486

Lai J, Wang G, Chai Y, Xin Y, Wu Q, Zhang X, Sun Y (2017). Deep burial diagenesis and reservoir quality evolution of high-temperature, high-pressure sandstones: examples from Lower Cretaceous Bashijiqike Formation in Keshen area, Kuqa Depression, Tarim Basin of China. AAPG Bull, 101(06): 829–862

Lai J, Wang G, Wang S, Cao J, Li M, Pang X, Zhou Z, Fan X, Dai Q, Yang L, He Z, Qin Z (2018). Review of diagenetic facies in tight sandstones: diagenesis, diagenetic minerals, and prediction via well logs. Earth Sci Rev, 185: 234–258

Lei B, Lu T, Wang D, Wang Y, Li S, Gu S (2010). Research on the sedimentary microfacies and diageneses of Ma 5 (1–4) submember in Jingbian gas field. Acta Sedimentologica Sinica, 28: 1153–1164

Li Z, Lin C, Dong B, Bu L (2012). An internal structure model of subaqueous distributary channel sands of the fluvial-dominated delta. Acta Petrol Sin, 33: 101–105

Li Y, Gao X, Meng S, Wu P, Niu X, Qiao P, Elsworth D (2019a). Diagenetic sequences of continuously deposited tight sandstones in various environments: a case study from upper Paleozoic sandstones in the Linxing area, eastern Ordos Basin, China. AAPG Bull, 103 (11): 2757–2783

Li Y, Yang J, Pan Z, Meng S, Wang K, Niu X (2019b). Unconventional natural gas accumulations in stacked deposits: a discussion of upper Paleozoic coal-bearing strata in the east margin of the Ordos Basin, China. Acta Geol Sin (English Edition), 93(1): 111–129

Li Y, Tang D, Wu P, Niu X, Wang K, Qiao P, Wang Z (2016) Continuous unconventional natural gas accumulations of Carboniferous-Permian coal-bearing strata in the Linxing area, northeastern Ordos Basin, China. Journal of Natural Gas Science & Engineering 36: 314–327 (in Chinese)

Liu C, Liu K, Wang X, Zhu R, Wu L, Xu X (2019). Chemo-sedimentary facies analysis of fine-grained sediment formations: an example from the Lucaogou Fm in the Jimusaer Sag, Junggar Basin, NW China. Mar Pet Geol, 110: 388–402

Liu J, Ding W, Dai J, Gu Y, Yang H, Sun B (2018) Quantitative multiparameter prediction of fault-related fractures:a case study of the second member of the Funing Formation in the Jinhu Sag, Subei Basin. Petroleum Science 15: 20–35

Liu Y, Xian C, Li Z, Wang J, Ren F (2020). A new classification system of lithic-rich tight sandstone andits application to diagnosis high-quality reservoirs. Geo-Energy Research, 4(3): 286–295 (in Chinese)

MacFadden B, Symister C, Cannarozzi N, Pimiento C, De Gracia C (2015). Comparative diagenesis and rare earth element variation in miocene invertebrate and vertebrate fossils from Panama. J Geol, 123(6): 491–507

Mao Y, Zhong D, Li Y, Yan T, Wang D, Liu Y, Lu Z (2016). Correlations and its controlling factors between porosity and permeability of the Cretaceous middle and deep buried sandstone reservoirs in Kuqa foreland thrust belt. Journal of China University of Mining & Technology, 45: 1184–1192 (in Chinese)

Marchand A, Smalley P, Haszeldine R, Fallick A (2002). Note on the importance of hydrocarbon fill for reservoir quality prediction in sandstones. AAPG Bull, 86: 1561–1571

Milliken K, Olson T (2017). Silica diagenesis, porosity evolution, and mechanical behavior in Siliceous mudstones, Mowry shale (Cretaceous), Rocky Mountains, U.S.A. J Sediment Res, 87(4): 366–387

Morad S, Al-Ramadan K, Ketzer J, DeRos L (2010). The impact of diagenesis on the heterogeneity of sandstone reservoirs: a review of the role of depositional facies and sequence stratigraphy. AAPG Bull, 94(8): 1267–1309

Mosavat N, Hasanidarabadi B, Pourafshary P (2019). Gaseous slip flow simulation in a micro/nano pore-throat structure using the lattice Boltzmann model. J Petrol Sci Eng, 177: 93–103

Net L, Alonso M, Limarino C O (2002). Source rock and environmental control on clay mineral associations, Lower Section of Paganzo Group (Carboniferous), Northwest Argentina. Sediment Geol, 152(3-4): 183–199

Qian W, Yin T, Hou G (2019). A new method for clastic reservoir

prediction based on numerical simulation of diagenesis: a case study of Ed1 sandstones in Bozhong depression, Bohai Bay Basin, China. Geo-Energy Research, 3(1): 82–93 (in Chinese)

Reza M (2018). The Assessment of microfacies and reservoir potential relationship (porosity and pore size) of the Sarvak Formation in SW Iran. Geosci J, 22(5): 793

Sallam E, Afife M, Fares M, van Loon A J, Ruban D A (2019). Sedimentary facies and diagenesis of the Lower Miocene Rudeis Formation (southwestern offshore margin of the Gulf of Suez, Egypt) and implications for its reservoir quality. Mar Geol, 413: 48–70

Sarkar S (2017). Microfacies analysis of larger benthic foraminifera-dominated Middle Eocene carbonates: a palaeoenvironmental case study from Meghalaya, N-E India (Eastern Tethys). Arab J Geosci, 10(5): 121

Shalaby M, Hakimi M H, Abdullah W H (2014). Diagenesis in the Middle Jurassic Khatatba Formation sandstones in the Shoushan Basin, northern Western Desert, Egypt. Geol J, 49(3): 239–255

Shi Z, Zhang Z, Ye H, Cai X, Sun J (2005). The mechanism of secondary pores in the reservoir of Funing Formation in Gaoyou Depression of Subei Basin. Acta Sedimentologica Sinica, 23: 429–436

Spotl C, Matter A, Brevart O (1993). Diagenesis and pore water evolution in the Keuper reservoir, Paris Basin (France). J Sediment Petrol, 63(5): 909–928

Tang J, Qi W, Peng L, Hao L, Tian B, Pang G (2013). Quantitative simulation of porosity-evolution in the Member 8 sandstone reservoir of the Yanchang formation in Huanxian Oilfield, Ordos Basin. Journal of Lanzhou University, 49: 320–326 + 331 (in Chinese)

Usman M, Siddiqui N, Zhang S, Ramkumar M, Mathew M, Sautter B, Beg M A (2020). Ichnofacies and sedimentary structures: a passive relationship with permeability of a sandstone reservoir from NW Borneo. J Asian Earth Sci, 192: 103992

Wang J, Cao Y, Xiao J, Liu K, Song M (2019). Factors controlling reservoir properties and hydrocarbon accumulation of the Eocene lacustrine beach-bar sandstones in the Dongying Depression, Bohai Bay Basin, China. Mar Pet Geol, 99: 1–16

Wang J, Zhang J, Xie J (2018a). Determination of the microstructure of a lithologic interface using the delayed response characteristics of horizontal well Gamma ray logging curves: a case study of the Daqingzijing Oilfield, Songliao Basin, northeast China. Arab J Sci Eng, 11(43): 6653–6664

Wang J, Zhang J, Xie J, Ding F (2014). Initial gas full-component simulation experiment of Ban-876 underground gas storage. J Nat Gas Sci Eng, 18: 131–136

Wang P, Jiang Z, Tang X, Li Z, Yuan Y, Zhang C (2015). Microscopic pore structure and heterogeneity quantitative characterization of shale reservoir-take in Chongqing southeast Longmaxi shale case. Acta Geol Sin, 89(s1): 91–92

Wang X, Hou J, Liu Y, Ji L, Sun J, Gong X (2018b). Impacts of the base-level cycle on pore structure of mouth bar sand bars: a case study of the Paleogene Kongdian Formation, Bohai Bay Basin, China. Energies, 11(10): 2617

Wu H, Zhang C, Ji Y, Liu R, Cao S, Chen S, Zhang Y, Wang Y, Du W, Liu G (2017). Pore-throat size characterization of tight sandstone and its control on reservoir physical properties:a case study of Yanchang Formation, eastern Gansu, Ordos Basin. Acta Petrol Sin, 38(8): 876–887

Yang R, Fan A, Han Z, Wang X (2012). Diagenesis and porosity evolution of sandstone reservoirs in the East II part of Sulige gas field, Ordos Basin. Int J Min Sci Technol, 22(3): 311–316

Yang Y, Sun G, Wang Y, Wu J, Jiang Y, Wang M, Li J (2020). Diagenesis and sedimentary environment of the lower Xiaganchaigou formation deposited during the Eocene/Oligocene transition in the Lenghu tectonic belt, Qaidam Basin, China. Environ Earth Sci, 79(10): 220

Yasin A, Ahmad A, Abdolkhalegh A (2019). Microfacies and depositional environment of Asmari formation in the Zeloi Oilfield, Zagros basin, south-west Iran. Carbonates Evaporites, 34(4): 1583–1593

Zhang K, Guo Y, Bai G, Wang Z, Fan B, Wu J, Niu X (2018). Pore-structure characterization of the Eocene Sha-3 sandstones in the Bohai Bay Basin, China. Energy Fuels, 32(2): 1579–1591

Zhang J, Li D, Jiang Z (2010). Diagenesis and reservoir quality of the fourth member sandstones of Shahejie formation in Huimin depression, eastern China. J Cent South Univ Technol, 17(1): 169–179

Zhang J, Sun Z, Liu L, Li Y (2019). Sedimentary model of K-successions sandstones in H21 area of Huizhou depression, Pearl River Mouth Basin, South China Sea. Open Geosci, 11(1): 997–1013

Zhang L, Li Z, Luo X (2020). Sedimentary-diagenetic characteristics and heterogeneity models of sandstone reservoirs: an example of Silurian Kalpintage Formation, northwestern Tarim Basin, China. Mar Pet Geol, 118: 104440

Zhao H, Zhang J, Li S, Li S, Zhou L, Jiang Y (2017). Sedimentary characteristics and evolution models of lower part of Minghuazhen Formation in Neogene system in oilfield A, Bohai Bay Basin. Journal of Jilin University, 47(4): 1021–1029 (in Chinese)

Zhou J, Lin C, Zhang X, Yao Y, Pan F, Yu H, Chen S, Zhang M (2011). Provenance system and sedimentary facies of the Member 1 of Paleogene Dainan Formation in Gaoyou Sag, Jiangsu Province. Journal of Palaeogeography, 13: 161–174 (in Chinese)

Zhong Y, Zhou L, Tan X, Guo R, Zhao L, Li F, Jin Z, Chen Y (2018). Characteristics of depositional environment and evolution of Upper Cretaceous Mishrif Formation, Halfaya Oil field, Iraq based on sedimentary microfacies analysis. J Afr Earth Sci, 140: 151–168

Zou N, Zhang D, Wu T, Shi J, Zhang S, Lu X (2015). Reservoir characteristics and controlling factors in the dolomitic clastic rocks of Fengcheng Formation in northwestern Juggar Basin. Natural Gas Geoscience, 26: 861–870 (in Chinese)